Kinetics and thermodynamics of the sorption of furaltadone from aqueous solutions on magnetic multi-walled carbon nanotubes

Xu Chen and Zhen-hu Xiong

ABSTRACT

Magnetic multi-wall carbon nanotubes (M-MWCNTs) were used as an adsorbent for removal of furaltadone from aqueous solutions, and the adsorption behaviors were investigated by varying pH, sorbent amount, sorption time and temperature. The results showed that the adsorption efficiency of furaltadone reached 97% when the dosage of M-MWCNT was 0.45 $g \cdot L^{-1}$, the pH was 7 and the adsorption time was 150 min. The kinetic data showed that the pseudo-second-order model can fit the adsorption kinetics. The sorption data could be well explained by the Langmuir model under different temperatures. The adsorption process was influenced by both intraparticle diffusion and external mass transfer. The experimental data analysis indicated that the electrostatic attraction and π–π stacking interactions between M-MWCNT and furaltadone might be the adsorption mechanism. Thermodynamic analysis reflected that adsorption of furaltadone on the M-MWCNT was spontaneous and exothermic. Our study showed that M-MWCNTs can be used as a potential adsorbent for removal of furaltadone from water and wastewater.

Key words | adsorption, furaltadone, kinetics, magnetic multi-walled carbon nanotubes, thermodynamics

Xu Chen (corresponding author)
Zhen-hu Xiong
Tianjin Chengjian University,
Tianjin Key Laboratory of Water Quality Science and Technology,
Tianjin 300384,
China
E-mail: *13821659895@163.com*

INTRODUCTION

Furaltadone is one of the nitrofuran antibiotics that has a good antibacterial action on *Escherichia coli* and salmonella (Vinas *et al.* 2007); it has also antibacterial effects on most Gram-positive bacteria and Gram-negative bacteria, and it has been used to treat systemic infections with the advantages of high efficacy and a broad antibacterial spectrum (Cooper *et al.* 2008). Moreover, it is a well known antibiotic in aquaculture and widely used to prevent bacterial infections to promote the growth of aquatic animals (Leston *et al.* 2011). However, the antibiotic is responsible for antibiotic resistance and residue in the aquaculture industry (Vass *et al.* 2008). Many studies suggest that furaltadone and its metabolites *in vivo* were poisonous (Barbosa *et al.* 2007), and transfer into the foodchain, causing harmful effects to the final eaters' health. At present, many countries, including the United States, Canada, the EU and China, have banned the use of the nitrofuran antibiotic in the aquaculture industry, while illegal use remains common in some countries and regions due to its better antibacterial properties and attractive price. Therefore, research on methods to remove furaltadone from environmental samples is of great importance. Unfortunately, to the best of our knowledge, few publications are available in the existing literature that discuss the removal of furaltadone contaminant from aqueous systems by adsorption.

Multi-walled carbon nanotubes (MWCNTs) are relatively new adsorbents, which have attracted extensive attention due to their unique physicochemical and electrical properties (Merkoci *et al.* 2005; Takagi *et al.* 2008); magnetic MWCNTs (M-MWCNTs) combine the advantage of high adsorbed amounts with magnetic separation (Fomkin 2009). This composite material has a high specific surface area, large microspore volume, and is easy to recover from water due to its magnetism.

In this work, M-MWCNTs were chosen as sorbent for the removal of furaltadone from aqueous solution. The adsorption kinetics, isotherms and thermodynamics of the adsorption of furaltadone by M-MWCNT were studied. The effects of contact time, temperature and pH were

doi: 10.2166/wst.2014.313

investigated, and the estimate of the adsorption parameters and sorption mechanisms were discussed.

EXPERIMENTAL

Reagents and materials

MWCNTs were purchased from Chengdu Organic Chemicals Co., Ltd, Chinese Academy of Sciences; inside diameter 5–10 nm, external diameter 10–20 nm, length 50 μm, specific surface area 200 m^2 g^{-1}, purity > 95% (all physical parameters of MWCNTs were provided by the manufacturer). Furaltadone ($C_{13}H_{16}N_4O_6$; MW 324.29; CAS: 3759-92-0; 98% purity) was purchased from Aladdin Industry Corporation (Shanghai, China), and its molecular structure is shown in Figure 1.

All chemicals were of analytical reagent grade or the highest purity available from Tianjin Jiangtian Chemicals Ltd (Tianjin, China). Experimental water throughout the study was deionized water. In addition, all glassware was soaked in dilute nitric acid for 12 h and finally rinsed three times with pure water prior to use.

Apparatus

The concentration of furaltadone solution was detected by UV-vis spectrophotometer (T6, Beijing Persee General Instrument Co., Ltd, Beijing, China). According to the experimental determination, the maximum absorption wavelength of furaltadone was 365 nm, detection linear range was 10–20,000 $\mu g \cdot L^{-1}$, detection limit was 320 $\mu g \cdot L^{-1}$. The size, morphology and structure of the M-MWCNTs were characterized by a scanning electron microscopy (SEM, JSM-6700F, JEOL Ltd, Tokyo, Japan) and transmission electron microscopy (TEM, JEM-2011, JEOL Ltd, Tokyo, Japan). The Fourier transform infrared (FTIR) spectroscopy was measured on a Nicolet 6700 FTIR Spectrometric Analyzer using KBr pellets (Thermo Fisher Scientific, Waltham, MA, USA). A PHBJ-260 model pH meter (Shanghai Precision Scientific Instrument Co., Shanghai, China) was used for measuring the pH of solutions.

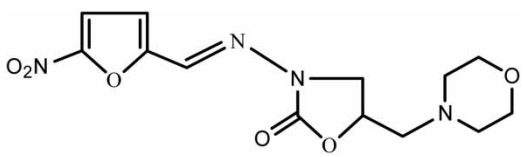

Figure 1 | The structure of furaltadone.

Synthesis of magnetic-modified multi-walled carbon nanotubes

The synthesis of M-MWCNTs was carried out according to the literature previously reported (Zhang *et al.* 2009). Typically, MWCNTs (1.5 g) were dissolved into a 250 mL round-bottom flask with 150 mL concentrated nitric acid, and stirred at 60 °C for 12 h. Then, the mixture was cooled to ambient temperature, washed with deionized water until the filtrate was neutral and finally dried under vacuum at 100 °C for 8 h. Subsequently, 1.0 g purified MWCNTs were dispersed in 200 mL purified water containing 4.33 mmol $(NH_4)_2Fe(SO_4)_2 \cdot 6H_2O$ and 8.66 mmol $NH_4Fe(SO_4)_2 \cdot 12H_2O$. The mixture was sonicated for 10 min and 10 mL 8 $mol \cdot L^{-1}$ ammonium hydroxide solution was then added dropwise into the solution under nitrogen gas, adjusting the pH of the mixture to 11–12. After that, the mixture was allowed to reflux for 30 min at 50 °C, and stirred at 300 rpm, while the suspension turned to black from brown. Then, the magnetic MWCNTs were separated from the suspension by magnet, washed three times with anhydrous alcohol and then three times with pure water, dried under vacuum at 40 °C, and finally placed in a desiccator for use in the next step.

Adsorption experiment

The adsorption percentage (Ads. %) was calculated according to the following equation:

$$\text{Ads.}\% = \frac{C_0 - C_t}{C_0} \times 100 \quad (1)$$

where C_0 and C_t are the initial (before adsorption) and the final (after adsorption) concentrations of furaltadone ($mg \cdot L^{-1}$), respectively. All adsorption tests were performed in triplicate to ensure the repeatability of the effect, based on the average of three measurements. All kinetic experiments were carried out at room temperature. Batch kinetic experiments were carried out by mixing 30.0 mg M-MWCNT and 50 mL of furaltadone solution with a known initial concentration (10, 20 and 30 $mg \cdot L^{-1}$) at natural pH and stirred in a shaker for different time intervals (2–240 min). The concentration of furaltadone left in the supernatant solution was analyzed as above.

Five different temperatures of 288, 293, 298, 303 and 308 K were applied to study the adsorption isotherm. The initial concentration of furaltadone varied from 8.0 to 20.0 $mg \cdot L^{-1}$. The amount of sorbent was kept constant

(30 mg). The thermodynamic parameters under different temperatures were recorded to analyze.

RESULTS AND DISCUSSION

Characterization of M-MWCNTs

MWCNT is a linear structure that winds together (Figure 2(a)); M-MWCNT is coated with ferroferric oxide nanometer particles (Figure 2(b)). It was observed that iron oxide black nanoparticles successfully coated the surface of MWCNT, and some of them went inside of MWCNT (Figure 2(d)). The reason was that capillary force overcame the surface tension of the water, leading Fe^{2+} and Fe^{3+} into the interior of MWCNT to produce black iron oxide (Zharikova *et al.* 2013). Furthermore, MWCNT was cut off by the oxidizing process of nitric acid to form the opening and the surface functional group, which helped the iron ion to go into the interior of MWCNT (Figure 2(d)).

The pH (pzc) of the M-MWCNT was determined by the following method: first, a series of 100 mL flasks containing 45 mL 0.1 mol·L^{-1} NaCl solutions was prepared. The initial pH (pH_i) value was adjusted in the range 2.0 to 10.0 by adding 0.1 mol·L^{-1} HCl or 0.1 mol·L^{-1} NaOH. The NaCl solutions (50 mL) were added to each flask. Then, a series of 0.10 g M-MWCNT was added to the flasks, which were stirred at 150 rpm for 48 h. The final pH values (pH_f) of the solutions were then detected. The pH_{PZC} was obtained with the plot of ΔpH (pH_i-pH_f) against pH_i. The pH(pzc) of M-MWCNT was the point of $\Delta pH = 0$. The pH_{PZC} of M-MWCNTs was 6.50 in our work (Figure 1S, available online at http://www.iwaponline.com/wst/070/313.pdf).

Effect of pH

The initial solution pH had a significant effect on the adsorption process. The removal efficiency of furaltadone reached a maximum when the solution pH was 7.0 (Figure 2S, available online at http://www.iwaponline.com/wst/070/313.pdf). Accordingly, the solution pH was adjusted to 7.0 in the following experiment. Moreover, under this condition, the removal rate of furaltadone decreased significantly from 99.2 to 58.6%, if the concentration of furaltadone solution increased from 10 to 30 mg·L^{-1}.

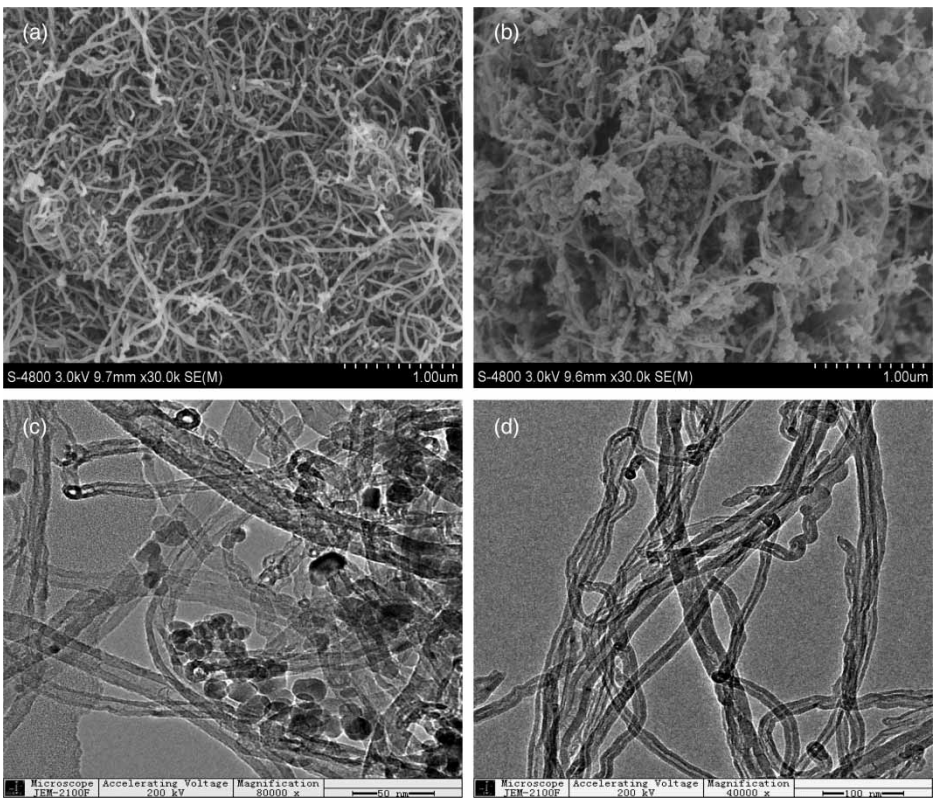

Figure 2 | SEM micrographs of MWCNTs (a), M-MWCNTs (b) and TEM micrographs of MWCNTs (c), M-MWCNTs (d).

The results indicate that the removal efficiency of furaltadone increased slightly with an increase of pH from acidic to neutral and reached the maximum at neutral pH value, when pH exceeded 7 there was a slight decrease in the uptake of furaltadone. This phenomenon was related to the amphoteric character of M-MWCNT surface and the pKa value for furaltadone. Generally, the pH of solution referred to its isoelectric point (pH_{PZC}), and the pH_{PZC} of M-MWCNTs was 6.50 (Figure 1S). At lower pH ($pH<pH_{PZC}$), the positive charge groups occupied the M-MWCNT surface and there was saturation of nitrogen atoms in the furaltadone molecule (Figure 1). The positive charge in the surface of the sorbent combined with the unshared pair electrons belonging to furaltadone due to electrostatic attraction (Chu *et al.* 2013), which promoted the removal efficiency of furaltadone. However, in the condition of pH< pKa (5.0) (Buzard & Conklin 1965), furaltadone is protonated and carries some positive charge, which may weaken the binding between adsorbent and adsorbate and lead to a slow and small increase of the removal efficiency. With the increase of the solution pH ($pH>pH_{PZC}$ and pH>pKa), the positive charge density in the surface of M-MWCNT decreased, and furaltadone formed anions by ionization at weak alkaline solution, which lead to an electrostatic repulsion phenomenon between the adsorbate and the adsorbent, which was unfavorable to the adsorption of furaltadone. However, under the circumstances, the non-electrostatic π-π dispersion interaction between bulk π systems on M-MWCNTs' surface and furaltadone molecules' unsaturated group (C=C, C=O), or hydrophobic interaction between M-MWCNT and furaltadone seems to be working and made the adsorbed amount of the nitrofuran antibiotics remain at a high level.

Effect of the amount of M-MWCNT

The percentages of furaltadone adsorbed increased over the range from 32.9 to 99.6% as the M-MWCNT dosage was increased from 0.05 to 0.60 $g \cdot L^{-1}$ (Figure 3S, available online at http://www.iwaponline.com/wst/070/313.pdf). The adsorption of furaltadone reached a plateau when M-MWCNT dosage was above 0.45 $g \cdot L^{-1}$, meanwhile, the removal efficiency held at 99.6% with almost no change. Therefore, 0.45 $g \cdot L^{-1}$ of M-MWCNT and 10.0 $mg \cdot L^{-1}$ of the furaltadone solution was the optimum amount for the adsorption in the research work. In the existing literature, it can be found that a high concentration of the adsorbent was not good for removing adsorbates from solutions in experiments to study the adsorption of reactive dyes by MWCNTs (Wu 2007). The reason was that a high concentration of MWCNT can increase the viscosity of the suspension and inhibit organic compound getting to the surface of MWCNT by molecular diffusion.

Adsorption kinetics

Adsorption kinetics is the most important characteristic of controlling the adsorption rate of solution, which represents the adsorption efficiency of the adsorbent. The effect of contact time on the removal of furaltadone is shown in Figure 3(a). Apparently, the adsorbed amount increased with increasing contact time, and reached equilibrium around 150 min. In addition, under the same concentration of the adsorbent, the adsorbed amount was correlated with the concentration of the adsorbate.

To investigate the amount of furaltadone adsorbed on the surface of the M-MWCNT at any time and equilibrium, the pseudo-first-order (2) and pseudo-second-order (3) models (Azizian 2004) were adopted to elucidate the adsorption kinetic process, which could be expressed as the following equations, respectively:

$$\ln(q_e - q_t) = \ln(q_e) - k_1 t \tag{2}$$

$$\frac{t}{q_t} = \frac{1}{k_2 q_e^2} + \frac{t}{q_e} \tag{3}$$

where q_e and q_t are the amounts of furaltadone adsorbed on the sorbent ($mg \cdot g^{-1}$) at equilibrium and at time t, respectively, and k_1 is the rate constant of the first-order adsorption (min^{-1}), k_2 is the rate constant of the second-order adsorption ($g \cdot mg^{-1} \cdot min^{-1}$). The values k_1 for furaltadone adsorption on M-MWCNT were determined from the plot of log (q_e–q_t) against t. The straight-line plots of t/q_t versus t have been tested to obtain rate parameters k_2. The pseudo-first-order and pseudo-second-order models fitting the adsorption of furaltadone on M-MWCNT at different concentrations are shown in Figure 3(b) and (c), respectively. The results of adsorption kinetics are shown in Table 1S (available online at http://www.iwaponline.com/wst/070/313.pdf). The correlation coefficient (R^2) of Equation (3) was more than 0.99, which is better than that of Equation (2), and the calculated q_e, which, depending on the pseudo-second-order model, was close to experiment data, indicating that the pseudo-second-order model fitted better to the adsorption process. Therefore, adsorption kinetics of furaltadone on M-MWCNT could be described by the pseudo-second-order model.

To evaluate the adsorption kinetics of furaltadone further, the Weber–Morris model (Equation (4)) and Boyd

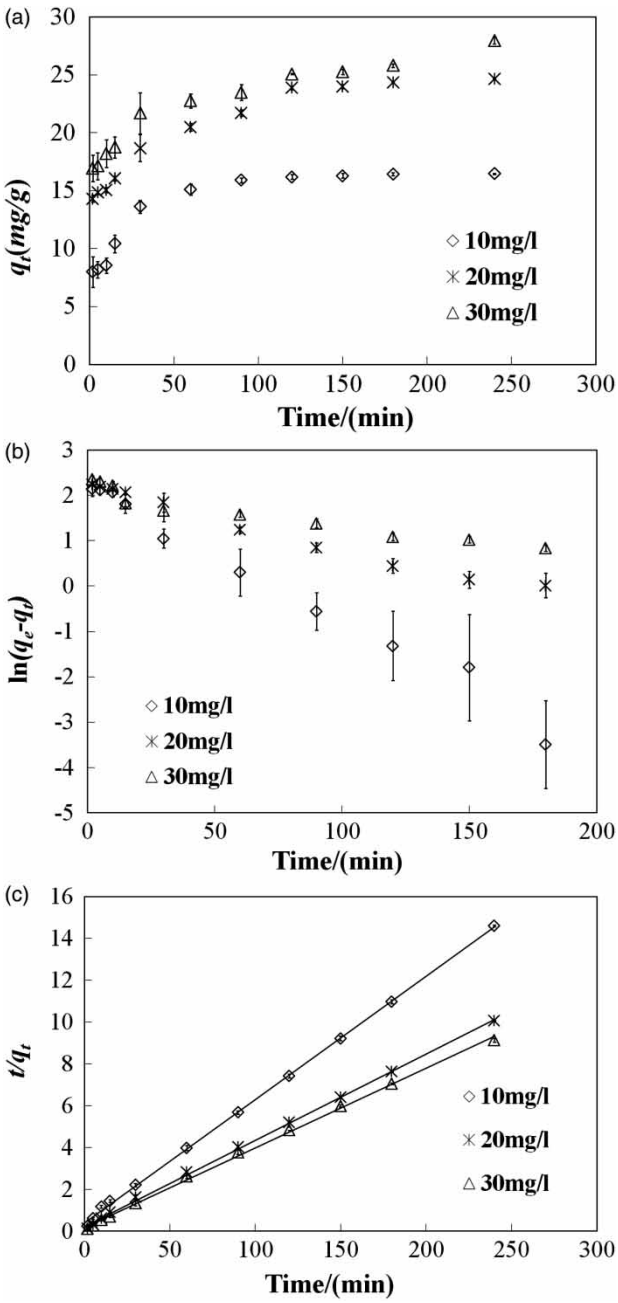

Figure 3 | Effect of contact time on the adsorption of furaltadone by MWCNT (a) and adsorption kinetics of furaltadone onto M-MWCNT at different concentrations fitted with pseudo-first-order (b) and pseudo-second-order (c).

model (Equation (5)) were applied to obtain the actual rate-controlling step involved in the furaltadone sorption process (Salam & Burk 2010):

$$q_t = K_d t^{1/2} + I \tag{4}$$

$$Bt = -\ln(1 - q_t/q_e) - 0.4977 \tag{5}$$

where q_t and q_e are the amounts of furaltadone adsorbed on M-MWCNT ($mg \cdot g^{-1}$) at time t (min) and equilibrium time (min), respectively. K_d is the rate constant for the intra-particle diffusion model ($mg \cdot g^{-1} \cdot min^{-1/2}$), values of I ($mg \cdot g^{-1}$) give an idea about the thickness of the boundary layer, and the larger the intercept, the greater the boundary layer effect will be. $B = \pi^2 D_i / r^2$ (Di is the effective diffusion coefficient of adsorbate and r is the radius of adsorbent particles assumed to be spherical). The values k_d and I were calculated from the slope and intercept of the straight line of q_t against $t^{1/2}$ as shown in Figure 4(a). The calculated Bt values were plotted against time t as shown in Figure 4(b).

As shown in Figure 4(a), these curves are multilinear, indicating that adsorption processes are affected by two or more steps. The first linear portion represented the initial adsorption process, in which the adsorbate got to the surface of the adsorbent driven by external diffusion. The second represented a relatively steady adsorption process, reflecting that the adsorbate had gone into the pores or bound to the inner surface of the adsorbent through the internal diffusion process. Moreover, the curve did not pass through the origin (Figuer 4(a)), suggesting that intraparticle diffusion is not the sole rate-controlling step (Lim *et al.* 2013). Therefore, the overall adsorption process was jointly controlled by intra-particle diffusion and external mass transfer.

The linearity of the plots provided useful information to distinguish between external mass transfer and intraparticle diffusion that control the mechanism of adsorption. As shown in Figure 4(b), the linear part did not pass through the origin, indicating that the adsorption process involved external mass transfer. But these lines were not strictly straight lines, meaning that the external diffusion of furaltadone uptake on M-MWCNT was fairly weak in rate control steps. This result verified the conclusion obtained in the Weber–Morris dynamic model.

Adsorption isotherms

The adsorption isotherm of M-MWCNT under different initial concentration is shown in Figure 5(a). The experimental data of equilibrium adsorption can be described by the Langmuir (Equation (6)) and Freundlich (Equation (7)) equations and the two models are represented, respectively, as follows (Chen *et al.* 2009):

$$\frac{C_e}{q_e} = \frac{C_e}{q_m} + \frac{1}{K_L q_m} \tag{6}$$

$$\ln q_e = \ln K_F + \frac{1}{n} \ln C_e \tag{7}$$

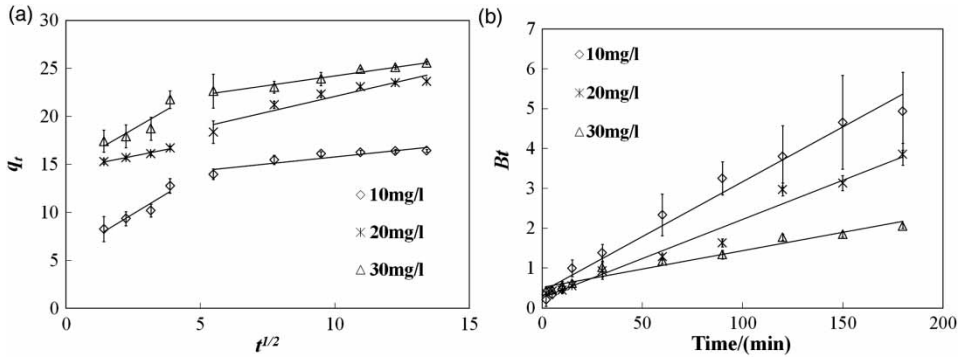

Figure 4 | Weber–Morris plots (a) and Boyd plots (b) for the adsorption of furaltadone onto M-MWCNT.

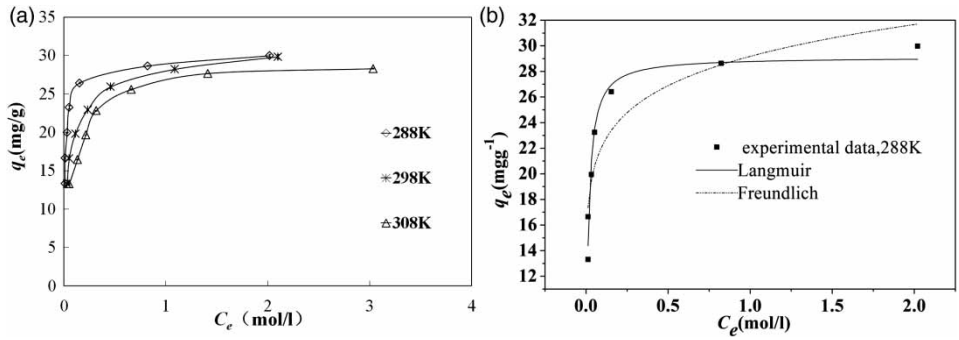

Figure 5 | Sorption isotherms of furaltadone onto M-MWCTs at different temperatures.

where q_m is the maximum monolayer adsorption ($mg \cdot g^{-1}$), C_e is the equilibrium concentration of furaltadone ($mg \cdot L^{-1}$), q_e is the amount of furaltadone adsorbed per unit weight of M-MWCNT at equilibrium concentration ($mg \cdot g^{-1}$) and K_L is the Langmuir constant related to the affinity of binding sites ($L \cdot mg^{-1}$). K_F is an empirical constant related to the sorption capacity of the adsorbent ($L \cdot mg^{-1}$), constant n is an empirical parameter.

Non-linear least-squares adjustments were applied to analyzing the data using Origin software (Figure 5(b)). The parameters of the Langmuir and Freundlich isotherm models are shown in Table 2S (available online at http://www.iwaponline.com/wst/070/313.pdf). Clearly, the Freundlich isotherms were not suitable evidenced from Figure 5 (b). Part of the reason is that the Freundlich model described reversible adsorption and was not restricted to the monolayer. Generally, the Langmuir isotherm is applied to homogeneous adsorption surfaces, whose adsorption sites have an equivalent affinity to the adsorbate, while the Freundlich isotherm was based on the adsorption process occurring on heterogeneous surfaces (Arasteh *et al.* 2010).

By comparing the residual sum of squares of the Langmuir model with that of the Freundlich model (Table 2S), it can be found that the latter is significantly larger than the former, indicating the energy distribution of the adsorption sites was homogeneous and that the Langmuir model fitted the experimental data better than the Freundlich model. Furthermore, the q_e value of furaltadone on M-MWCNT decreased with increasing temperature (Figure 5 (a)), indicating that raising the temperature was not favorable to the adsorption of furaltadone by M-MWCNT; on the contrary, low temperature was more favorable. In addition, the K_L, K_F and n values (Table 3S, available online at http://www.iwaponline.com/wst/070/313.pdf) decreased with increasing temperature, and so does the q_m value. All of this suggested that raising the temperature was not favorable to the adsorption of furaltadone. The parameter n relating to the intensity of sorption in the Freundlich model varied from large to small with the change of the surface heterogeneity and affinity.

The essential feature of the Langmuir isotherm expressed by means of the R_L, a dimensionless constant, is

related to the separation factor or equilibrium parameter. R_L is calculated as follows (Xu *et al.* 2008):

$$R_L = \frac{1}{1 + K_L C_0} \tag{8}$$

where C_0 is the initial furaltadone concentration ($mg \cdot L^{-1}$) and K_L is the Langmuir adsorption equilibrium constant ($L \cdot mg^{-1}$). The value of R_L expresses the shape of isotherm and indicates whether the binding of furaltadone onto M-MWCNT is favorable or not, according to the following indexes: unfavorable ($R_L > 1$), linear ($R_L = 1$), favorable ($0 < R_L < 1$), or irreversible ($R_L = 0$) (Fasfous *et al.* 2010). The R_L values in this work were found to be 0.005, 0.013 and 0.016 at 288, 298 and 308 K, respectively, indicating that the sorption of furaltadone is favorable.

Thermodynamic analysis

Thermodynamic parameters were calculated as follows:

$$\Delta G^0 = -RT \ln K_c \tag{9}$$

where R is the universal gas constant ($8.314\ J \cdot mol^{-1} \cdot K^{-1}$), T is the temperature (K) and K_c is the distribution coefficient. Gibbs free energy change of adsorption (ΔG^0) was calculated using $\ln K_c$ values for different temperatures. The K_c value was calculated using the following equation (Shen *et al.* 2009):

$$K_c = \frac{q_e}{C_e} \tag{10}$$

where C_e is the equilibrium concentration of furaltadone and q_e is the amount of furaltadone adsorbed per unit weight of M-MWCNT at equilibrium concentration ($mg \cdot g^{-1}$).

The enthalpy change (ΔH^0) and entropy change (ΔS^0) of adsorption were calculated as follows:

$$\ln K_c = \frac{\Delta S^0}{R} - \frac{\Delta H^0}{RT} \tag{11}$$

According to Equation (11), ΔH^0 and ΔS^0 parameter can be calculated from the slope and intercept of the plot of $\ln K_c$ versus $1/T$, respectively.

The thermodynamic parameters are listed in Table 3S. It is clear that the ΔH^0 and ΔG^0 values are both negative, which shows the exothermic and spontaneous nature of the sorption process. And this phenomenon was consistent with the result that raising the temperature was not favorable to the adsorption of furaltadone by M-MWCNT. ΔS^0 did not change with temperature under the research range of any temperature, indicating that randomness of the reaction did not change with temperature, and the negative values of ΔS^0 suggested randomness of the reactants decreased in the adsorption process. However, ΔG^0 changed with increasing temperature, leading to a favorable reduction through the adsorption process. In addition, according to ΔG^0 value, one can make sure that the type of adsorption process, such as 0–20 $kJ \cdot mol^{-1}$ is physical adsorption and -80 to 400 $kJ \cdot mol^{-1}$ is chemical adsorption (Chen *et al.* 2007), respectively. In this study, the magnitude of ΔG^0 ranged from 0–20 $kJ \cdot mol^{-1}$ indicating that the adsorption process is mainly driven by physical properties.

CONCLUSION

The adsorption behavior of furaltadone on M-MWCNT was researched in this article. The adsorbed amount increased with the increase of initial concentration of furaltadone and interaction time, but decreased with the increase of temperature and pH value (>7) of the solution. The adsorption capability reached equilibrium within 150 min, and the removal efficiency was 97%. The kinetics of M-MWCNT-bound furaltadone follows the pseudo-second-order model. The Langmuir model fitted the experimental data better than the Freundlich model. The negative ΔG^0 shows that the adsorption process was spontaneous and exothermic. The adsorption mechanism may be the action of π–π electron donor-receptor; it was a crucial driving force in the adsorption of organic compounds on MWCNT. The results showed that M-MWCNTs have a potential applicability to removing furaltadone from water.

ACKNOWLEDGEMENTS

This research was supported by the National Nature Science Foundation of China (grant number: 50878138). We thank our colleagues and other students who participated in this work.

REFERENCES

Arasteh, R., Masoumi, M., Rashidi, A. M., Moradi, L., Samimi, V. & Mostafavi, S. T. 2010 Adsorption of 2-nitrophenol by

multi-wall carbon nanotubes from aqueous solutions. *Applied Surface Science* **256** (14), 4447–4455.

Azizian, S. 2004 Kinetic models of sorption: a theoretical analysis. *Journal of Colloid and Interface Science* **276** (1), 47–52.

Barbosa, J., Ferreira, M. L., Ramos, F. & Silveira, M. I. N. 2007 Determination of the furaltadone metabolite 5-methylmorpholino-3-amino-2-oxazolidinone (AMOZ) using liquid chromatography coupled to electrospray tandem mass spectrometry during the nitrofuran crisis in Portugal. *Accreditation and Quality Assurance* **12** (10), 543–551.

Buzard, J. A. & Conklin, J. D. 1965 A comparison of the concentrations of certain nitrofurans in the aqueous humour and cerebrospinal fluid of the dog. *British Journal of Pharmacology* **24**, 266–273.

Chen, G.-C., Shan, X.-Q., Zhou, Y.-Q., Shen, X.-e., Huang, H.-L. & Khan, S. U. 2009 Adsorption kinetics, isotherms and thermodynamics of atrazine on surface oxidized multiwalled carbon nanotubes. *Journal of Hazardous Materials* **169** (1–3), 912–918.

Chen, W., Duan, L. & Zhu, D. 2007 Adsorption of polar and nonpolar organic chemicals to carbon nanotubes. *Environmental Science & Technology* **41** (24), 8295–8300.

Chu, Y., Li, X., Xie, H., Fu, Z., Yang, X., Qiao, X., Cai, X. & Chen, J. 2013 Evaluating the interactions of organic compounds with multi-walled carbon nanotubes by self-packed HPLC column and linear solvation energy relationship. *Journal of Hazardous Materials* **263**, 550–555.

Cooper, K. M., McCracken, R. J., Buurman, M. & Kennedy, D. G. 2008 Residues of nitrofuran antibiotic parent compounds and metabolites in eyes of broiler chickens. *Food Additives and Contaminants* **25** (5), 548–556.

Fasfous, I. I., Radwan, E. S. & Dawoud, J. N. 2010 Kinetics, equilibrium and thermodynamics of the sorption of tetrabromobisphenol A on multiwalled carbon nanotubes. *Applied Surface Science* **256** (23), 7246–7252.

Fomkin, A. A. 2009 Nanoporous materials and their adsorption properties. *Protection of Metals and Physical Chemistry of Surfaces* **45** (2), 121–136.

Leston, S., Nunes, M., Viegas, I., Lemos, M. F. L., Freitas, A., Barbosa, J., Ramos, F. & Pardal, M. A. 2011 The effects of the nitrofuran furaltadone on *Ulva lactuca*. *Chemosphere* **82** (7), 1010–1016.

Lim, C. K., Bay, H. H., Neoh, C. H., Aris, A., Abdul Majid, Z. & Ibrahim, Z. 2013 Application of zeolite-activated carbon macrocomposite for the adsorption of Acid Orange 7: isotherm, kinetic and thermodynamic studies. *Environmental Science and Pollution Research Institute* **20** (10), 7243–7255.

Merkoci, A., Pumera, M., Llopis, X., Perez, B., del Valle, M. & Alegret, S. 2005 New materials for electrochemical sensing VI: Carbon nanotubes. *TrAC Trends in Analytical Chemistry* **24** (9), 826–838.

Salam, M. A. & Burk, R. C. 2010 Thermodynamics and kinetics studies of pentachlorophenol adsorption from aqueous solutions by multi-walled carbon nanotubes. *Water Air and Soil Pollution* **210** (1–4), 101–111.

Shen, X.-E., Shan, X.-Q., Dong, D.-M., Hua, X.-Y. & Owens, G. 2009 Kinetics and thermodynamics of sorption of nitroaromatic compounds to as-grown and oxidized multiwalled carbon nanotubes. *Journal of Colloid and Interface Science* **330** (1), 1–8.

Takagi, A., Hirose, A., Nishimura, T., Fukumori, N., Ogata, A., Ohashi, N., Kitajima, S. & Kanno, J. 2008 Induction of mesothelioma in p53 +/− mouse by intraperitoneal application of multi-wall carbon nanotube. *Journal of Toxicological Sciences* **33** (1), 105–116.

Vass, M., Hruska, K. & Franek, M. 2008 Nitrofuran antibiotics: a review on the application, prohibition and residual analysis. *Veterinarni Medicina* **53** (9), 469–500.

Vinas, P., Campillo, N., Carrasco, L. & Hernandez-Cordoba, M. 2007 Analysis of nitrofuran residues in animal feed using liquid chromatography and photodiode-array detection. *Chromatographia* **65** (1–2), 85–89.

Wu, C.-H. 2007 Adsorption of reactive dye onto carbon nanotubes: Equilibrium, kinetics and thermodynamics. *Journal of Hazardous Materials* **144** (1–2), 93–100.

Xu, D., Tan, X., Chen, C. & Wang, X. 2008 Removal of Pb(II) from aqueous solution by oxidized multiwalled carbon nanotubes. *Journal of Hazardous Materials* **154** (1–3), 407–416.

Zhang, Q., Zhu, M., Zhang, Q., Li, Y. & Wang, H. 2009 The formation of magnetite nanoparticles on the sidewalls of multi-walled carbon nanotubes. *Composites Science and Technology* **69** (5), 633–638.

Zharikova, E. F., Ochertyanova, L. I., Vasylenko, I. V., Dobrokhotova, Z. V., Bogomyakov, A. S., Imshennik, V. K., Maksimov, Y. V., Kiskin, M. A., Ivanov, V. K., Kirdyankin, D. I., Shub, B. R., Grishin, M. V., Ganin, A. K., Novotortsev, V. M. & Eremenko, I. L. 2013 New magnetic material based on modified multi-walled carbon nanotubes and iron(III) derivatives. *Russian Chemical Bulletin* **62** (3), 646–656.

First received 15 April 2014; accepted in revised form 30 June 2014. Available online 10 July 2014